BALLISTIC RESEARCH LABORATORIES

REPORT NO. X-127

Explosion of Spherical Charges in Air: Travel Time, Velocity of Front, and Duration of Shock Waves

(Detonation av klotformiga laddningar i luft; gångtid, fronthastighet och våglängd hos den utsända stötvågen)

PROF. WALODDI WEIBULL

Tidskift for kustartilleriet
(Coastal Artillery Journal)
No. 1, 1947

A Translation by LARS NICLAS ENEQUIST

with two Appendices:

(A) Translation of L. I. Sedov's paper
"Le mouvement d'air en cas d'une forte explosion"

(B) Comparison of Data Compiled at Aberdeen with Data of Weibull's paper

ABERDEEN PROVING GROUND, MARYLAND

B A L L I S T I C R E S E A R C H L A B O R A T O R I E S

REPORT NO. X-127

Explosion of Spherical Charges in Air: Travel Time, Velocity of Front, and Duration of Shock Waves

(Detonation av klotformiga laddningar i luft: gångtid, fronthastighet och våglängd hos den utsända stötvågen)

Prof. Waloddi Weibull

Tidskift for kustartilleriet
(Coastal Artillery Journal)
No. 1, 1947

A Translation
by

Lars Niclas Enequist

with two Appendices:

(A) Translation of L. I. Sedov's paper "Le mouvement d'air en cas d'une forte explosion"

(B) Comparison of Data Compiled at Aberdeen with Data of Weibull's paper

February 1950

A B E R D E E N P R O V I N G G R O U N D, M A R Y L A N D

CONTENTS

Note:

Translator's remarks are inclosed by brackets.

INTRODUCTION

It has long been known that a shock wave is propagated in a gas with a velocity which changes with pressure and which may be many times greater than the velocity of sound. Accordingly, the velocity is measured by the pressure and the energy content in the wave, and is, therefore, a rather significant factor in the determination of the demolition capacity of the wave. Nevertheless, knowledge regarding shock velocity is quite incomplete and unsatisfactory despite the many investigations carried out in the past.

The measurements presented here were made at the Fysikaliska Forskningsavdelningen vid AB Bofors [Physical Research Department at Bofors, Ltd.] , and aim to cope directly with this deficiency regarding spherical charges.

Knowledge of the results also yields the opportunity to check theory by examining the connexion between the emanating wave and the characteristics of the explosive charge. This was another reason for the present rather comprehensive investigation.

We were particularly anxious to check two theories: an old one by Rüdenberg (Reference 1), and a quite recent one by Sedov (Reference 2) because of application to the calculation of the amount of energy that is liberated by an atomic bomb explosion. Below are shown the Bofors measurements which are not at all in agreement with the predictions of either of the above theories. Thus it is certain that the above theories are useless for the calculation of the amount of energy liberated by an atomic bomb explosion. Applications to the atomic bomb appear, therefore, to be hardly promising.

Let us survey the previous experimental work published on this topic. One then meets only with qualitative results. Many investigators have found that shock front velocity is very high in the vicinity of the charge and that it decreases with distance, gradually approaching acoustic velocity, and from their findings have attempted to formulate laws, but the measurements turned out to be irreproducible.

The essential cause of the poorness of these results, despite the range of weights of charges exploded, which in some cases extended up to 1500 kg, is indubitably due to the neglect of the effect of the shape of the charge. Measurements at Bofors have shown that cylindrical charges produce a distinct directional effect not only with respect to the impulse, as the author has demonstrated in Reference 3, but also with regard to the velocity. Thus it is apparent that when velocity measurements are obtained without consideration of the shape of the charge, the results will be rather puzzling and irreproducible. This remark applies to all the experiments carried out by the authors named below. It should further be added that the charges were often inserted in magazine containers or metallic covers which could have directed the explosion wave in an imperspicuous manner.

The first velocity measurements of explosion waves were made by Mach, who, in 1877 to 1889, experimented with very small charge weights. Among other experiments we may list those by Wolff (Reference 4), von Angerer and Ladenburg (Reference 5), Burlot (Reference 6), and Partlo and Service (Reference 7).

The two last named experimenters have made the notable observation that the velocity within a certain range of charge radii is subsonic. It does not appear likely that this result is correct. Apparently, the error lies in the neglect of the directional effect and of the scaling law derived from the principle of dynamic similarity according to which all velocities are equal at distances measured in charge radii, for a specified type of explosive.

The form of the charge introduces considerable complications as to the directional effect, particularly near the ground. It is reasonable to begin by eliminating these difficulties by choosing as a charge form the sphere which alone is fully symmetric if set off at the charge centre. This is the reason for confining the present investigation to spherical charges.

When such a charge is detonated it sends out a shock wave within which the pressure behaves, as Figure 1 shows, with a pressure maximum at the discontinuous front. The pressure generally decreases linearly with time behind the front and attains at point 2 the value of one atmosphere to drop below this value thereafter. The wave front is propagated with a velocity w_1 which decreases with the distance from the charge, starting from the maximum value w_o at the surface.

R_o = charge radius

R = distance from the centre of the charge

T_1 = time for shock front to reach R, starting from R_o

T_2 = time for pressure to become atmospheric after passage of the shock front

Q = charge weight

w_2 = shock velocity at time T_2.

Then the corresponding quantities scaled according to the law of similitude are:

$$r = R\,Q^{-1/3}, \qquad r_o = R_o Q^{-1/3}$$

$$t_1 = T_1 Q^{-1/3}, \qquad t_2 = T_2 Q^{-1/3}.$$

The times t_1 and t_2 are related to r and r_o by

$$t_1 = f_1(r - r_o), \quad t_2 = f_2(r - r_o)$$

where f_1 and f_2 depend on the type of explosive but do not depend explicitly on Q.

FIG. 1

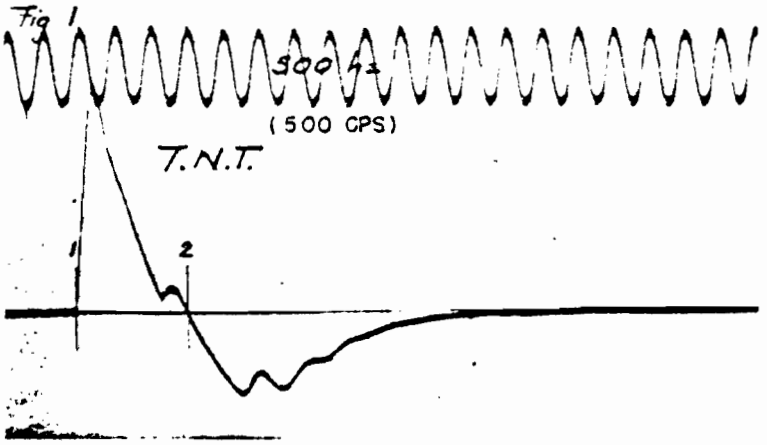

Pressure-Time Curve for Spherical TNT Charges

FIG. 2

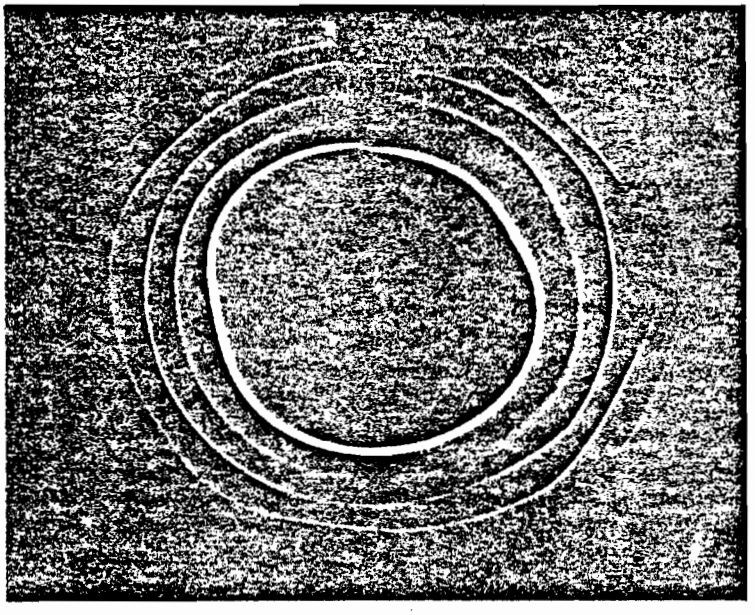

Typical Cathode-Ray Oscillogram Showing Measured Time Intervals

FIG. 3

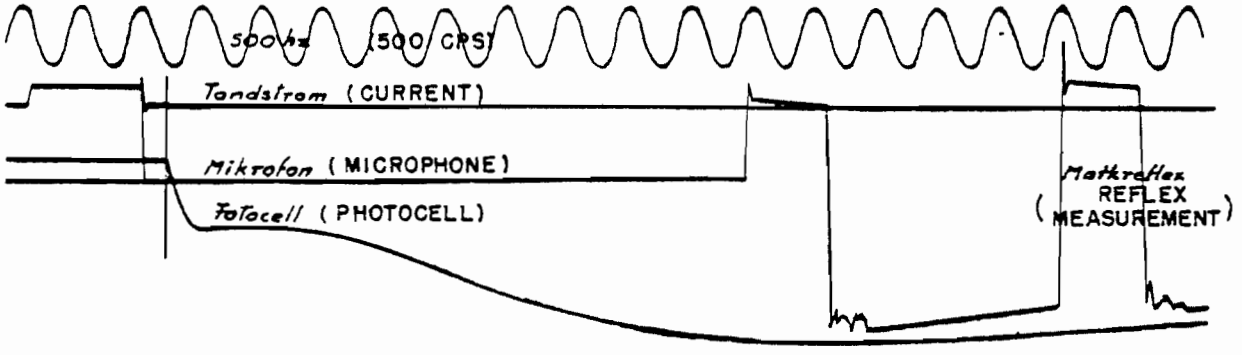

Oscillogram with Curve Distorted for Time Measuring

The difference $t_+ = t_2 - t_1$ is the duration of the positive pressure at a fixed point r while a wave is passing. The positive wave-length l_+ is the distance between the position of the front at time t_2 and r. One then gets

$$l_+ = w_2(t_2 - t_1), \quad \left[\text{sic; } l_+ = \frac{w_1 + w_2}{2}(t_2 - t_1) \text{ is a better approximation}\right]$$

where w_2 may approximately be replaced by the sonic velocity c_o at large distances.

EXPERIMENTAL PROCEDURE

At the moment the explosion products break through the surface of the charge, almost immediately a shock wave forms and an intensive radiation is emitted and is recorded on an oscillograph by means of a highly evacuated photocell (Philips, type 3250) and a trigger coupling. At the distance R is placed a crystal-receiver which registers the time of arrival of the wave at R.

The arrangements have to be varied according to whether the distance is small or large because in the former case one measures time of the order of microseconds and excess pressures that are exceedingly high, while in the latter case one measures longer time intervals of the order of milliseconds and smaller excess pressures.

At small distances one uses an S.K. quartz-gauge. It consists of a steel rod, at the farthest end of which one places a quartz crystal shielded by a threaded hood. The oscillograph is a polar-recording cathode-ray oscillograph built by the Fysikaliska Forskingsavdelningen, AB Bofors which contains a cathode-ray tube manufactured by the AB Standard Radio Fabrik, Stockholm. Spots of light describe a spiral consisting of about three effective turns with a speed that is adjustable in steps from 20.000 to 200 rps. For a shorter time interval a higher speed of rotation of the oscillograph trace is used. Thus certain difficulties arise on how to start the oscillograph at the right moment so that one loses the incoming signals from neither the photocell nor the quartz-gauge. These signals are, as a rule, three in number, taken at various distances from the charge. Thus three travel times are measured for each explosion. The problem is solved in the following manner: The charge is initiated by a detonator cap and a PETN-fuze* through which a thin copper thread is drawn out to a suitable distance from the explosive cap. When this wire breaks, the oscillograph commences to sweep its spiral path, which is recorded on the screen. Using various lengths for the fuze between the break-wire and the detonator cap in the centre of the charge one may easily reproduce various delay times. Such an oscillogram is shown in Figure 2. The oscillograph tubes do not indicate full circular symmetry. Therefore, the reading is performed with the aid of a calibrated protractor. With a speed of 10.000 rps the reading accuracy is about 0.5 μs, i.e., one may measure 50 μs with a tolerance of 1 per cent.

* $\left[\text{PETN} = C_5H_8O_{12}N_4\right]$

Of course, it is important for such short time intervals that the response time of the entire circuit be minimal. This requirement is checked by firing several shots with a quartz crystal cemented directly to the surface of the charge at each firing. The signal from the crystal and the photocell trigger circuit are incorporated simultaneously in the cathode-ray oscillograph which has a recording velocity of 4000 m sec.$^{-1}$. It turned out that the time difference between the two signals maintained the magnitude of 1 to 2 times 10^{-7} sec., i.e., a value safely below the accuracy of reading.

At large distances a six-spiral Siemens oscillograph was employed with a maximal paper speed of 10 m sec^{-1}. The crystal receiver was a Brush microphone with Seignette crystal. The microphone is connected to a non-linear amplifier, that is, one with very high sensitivity for small input voltage, but with current saturation already at moderate voltage [i.e., a high gain amplifier]. Accordingly, zero time in the pressure-time curve may be measured with an accuracy greater than the one obtainable with the use of a linear amplifier. For this compare Figure 3 which shows the distorted and normal diagrams according to Figure 1. The current curve of the photocell is also shown in the figure. In order to facilitate distance measurements and to reduce effects of possible horizontal wind disturbances the charge is suspended vertically above the microphone placed about 1 m above the ground. Time measurements are made with a tuning fork calibrated with one from the Telegraph Company at a telephonically transmitted frequency of 500 Hz [i.e., cps], the accuracy of which is indicated to be greater than 1 in 10^5.

Explosions in compressed and evacuated air are carried out in a specially constructed spherical chamber of 5.5 m^3 displacement with a diameter of 2 m. This permits the explosion of 0.25 kg of TNT [= $C_7H_5O_6N_3$] at an initial pressure or 4 ata [atmospheres absolute]. The container can also be evacuated to a vacuum of a few mm Hg. The measuring arrangements are the same as given above for small distances in free air. The photocells are located outside the container and react to the radiation from within through a small glass window. Quartz-gauges are placed inside the chamber and are connected by pressure-sealed leads to each of their trigger circuits on the outside.

EXPERIMENTAL RESULTS AND CORRECTIONS

Charges are weighed in grams, small distances are measured in millimeters, and large distances in centimeters. Temperature, humidity and barometric pressure are determined before every shot. The charges are exploded in calm air.

The measurements are corrected as follows:

1. Quartz-gauge measurements of travel times are decreased by 1 μs corresponding to the time the pressure requires to be transmitted through the protective shield of the gauge.

2. Travel times are reduced to a temperature of 0 deg C and a humidity of 0 per cent by multiplication by the factor

$$k = 1 + 1.832 \times 10^{-3} \vartheta + 0.16\, eh/B$$

where

ϑ = temperature in deg C,

e = humidity in per cent,

h = measured vapour pressure,

B = barometric pressure.

The factor k indicates the ratio of sonic velocity in the given still atmosphere to that in an atmosphere of 0 deg C and 0 per cent humidity.

3. The times measured by the polar-recording oscillograph are reduced by 0.89 per cent because it permits agreement with the more accurately calibrated time indication of the spiral oscillograph.

The parameters varied within the following limits:

Temperature	2.5 to 21.2 deg C,
Humidity	61 to 96 per cent,
Barometric Pressure	738 to 759 mm Hg,
Charge Weight	0.246 to 0.255 kg,
	0.965 to 1.005 kg.
Type of Explosive	PETN; TNT with 10, 20, 30 per cent Al.

The corrected mean values of the times are found in Tables I to III as follows:

Table I gives the times t_1 and t_2 at atmospheric pressure.

Table II gives the times t_1 at various densities of the ambient air,

Table III gives the times t_1 at atmospheric pressure for explosive charges other than 100 per cent TNT, namely: PETN; TNT with 10, 20, 30 per cent Al.

With the few measurements that we have for any given distance it would be unreasonable to calculate the mean square error. As a measure of dispersion we choose instead the differences between the highest and the lowest measured values (the range). The greatest deviations from the above mean values, given in columns 2 and 4, are thus approximately one-half of the range quoted in columns 3 and 5.

The dispersion in r varies with the charge weight.

TABLE I

MEASURED TIME FOR SHOCK FRONT TO REACH r, AND TIME AT WHICH THE EXCESS PRESSURE VANISHES

Values corrected to 1 kg charge weight, 0 deg C temperature, and 0 per cent humidity.

Explosive Charge: TNT.

$r_o = 0.054$ m $kg^{-1/3}$.

Q = 0.25 kg					Q = 1.00 kg				
1	2	3	4	5	6	7	8	9	10
No. of Obs.	$r - r_o$ m*	Dispersion mm	t ms	Dispersion μs	No. of Obs.	$r - r_o$ m	Dispersion mm	t ms	Dispersion μs
Small Distance: Wave Front									
4	.104	1	.021	1	4	.200	1	.047	2
4	.183	1	.043	6	4	.300	1	.083	2
4	.341	2	.100	7	4	.400	1	.128	6
1	.422	-	.133	-	5	.446	2	.142	30
6	.579	1	.213	16	5	.546	3	.204	19
5	.658	4	.264	17	5	.746	4	.341	21
6	.737	4	.330	21	4	.846	6	.418	15
5	.816	4	.389	8	4	1.046	2	.611	0
6	.897	6	.465	27	4	1.246	1	.843	20
7	1.056	12	.626	31					
5	1.215	14	.809	48					
7	1.374	15	1.018	28					
5	1.532	10	1.224	21					
6	1.690	12	1.491	43					
5	1.848	13	1.774	24					
1	2.001	--	2.062	--					
Large Distance: Wave Front									
2	3.11	10	4.41	90	2	3.95	10	6.54	30
2	6.22	20	12.72	0	3	5.98	30	12.04	10
3	9.44	0	21.79	40	2	7.97	10	17.33	40
2	12.57	10	30.68	60	2	9.93	20	22.97	30
2	15.74	0	39.81	25	2	11.94	0	28.97	40
2	18.85	0	49.22	24					
Large Distance: Time at which Positive Phase Vanishes for Given Distance r									
2	12.57	10	34.90	140	2	7.97	10	20.95	450
2	15.74	0	44.37	490	2	9.93	20	27.00	90
2	18.85	0	53.65	190	2	11.94	0	32.75	70

* [sic; the dimensions given in this row should be multiplied by $kg^{-1/3}$]

TABLE II

SHOCK FRONT TRAVEL TIME MEASURED AT VARIOUS AMBIENT DENSITIES

Values corrected to 1 kg charge weight, 0 deg C temperature, and 0 per cent humidity. Density ϱ_o - in kg m^{-3}.

Explosive Charge: TNT.

Charge weight: 0.25 kg.

$r_o = 0.054$ m $kg^{-1/3}$.

$r - r_o$	$Q_o = 5.10$		$Q_o = 3.81$		$Q_o = 2.55$		$Q_o = 1.20$	
	μs*	%	μs	%	μs	%	μs	%
.158	50.6	146	45.8	132	40.8	118	34.6	100
.278	--	---	99.9	136	--	---	73.5	100
.316	131.7	149	121.3	137	105.9	120	88.2	100
.342	147.6	149	136.4	138	--	---	98.8	100
.476	249.0	153	229.1	141	202.0	124	162.6	100
.786	584.0	159	534.6	145	--	---	368.1	100

The travel times are measured by one shot for each distance, except for $\varrho_o = 2.55$ where two shots are used, and $\varrho_o = 1.29$ where the times are calculated by the formulae for small distances.

TABLE III

MEASURED TRAVEL TIMES FOR VARIOUS EXPLOSIVE CHARGES COMPARED TO THOSE FOR TNT AT ATMOSPHERIC PRESSURE

Mean values of two shots at each distance.

$r - r_o$ m**	PETN %	10 % Al + 90 % TNT %	20 % Al + 80 % TNT %	30 % Al + 70 % TNT %
.26	95	100	104	111
.50	94	107	102	112
.74	94	101	101	107
1.05	94	100	105	103
1.35	94	99	95	101
1.65	100	100	100	103
M. v.	95	101	104	114
k_o	93	104	104	114
k_1	+.03	-.03	-.03	-.03

* [sic; μs . $kg^{-1/3}$ in this row]

** [sic; m . $kg^{-1/3}$]

EVALUATION OF EXPERIMENTAL RESULTS

The measured values of the travel times t_1 and t_2 may be reproduced very accurately by means of the following formulae:

For small distances

$$t_1 = b_o(r - r_o) + b_1(r - r_o)^2 + b_2(r - r_o)^3;$$

For large distances

$$1/t_2 = c_o/(r - r_o) + c_1/(r - r_o)^2$$

where c_o is the sonic velocity, i.e., 33.3 m sec.$^{-1}$ [sic; 331.3 m sec^{-1}]. The b's and c's are determined by the method of least squares.

Thus the following values are obtained for a spherical TNT charge:

$$b_o = 0.1614, \qquad b_1 = 0.3598, \qquad b_2 = 0.0390;$$

$$c_o = 331.3, \qquad c_1 = 376.7.$$

It is evident from Figures 4 and 5 that the measured times fall on the curve computed from the above formula quite well, and that values for various charge weights lie on the same curves since they are reduced in conformance with the laws of similitude the validity of which is thus confirmed in this particular case.

The velocity for large distances is calculated from the measured travel times by the method of Partlo and Service (Reference 7).

One calculates the difference Δ between the travel times of the sound wave ($c = 331.3$ m sec^{-1}) and the shock wave as follows:

$$\Delta = (r - r_o)/c - t.$$

Differentiating, one obtains

$$d\Delta/dr = 1/c - 1/w$$

whence

$$w = c/\left[1 - c(d\Delta/dr)\right].$$

FIG. 4

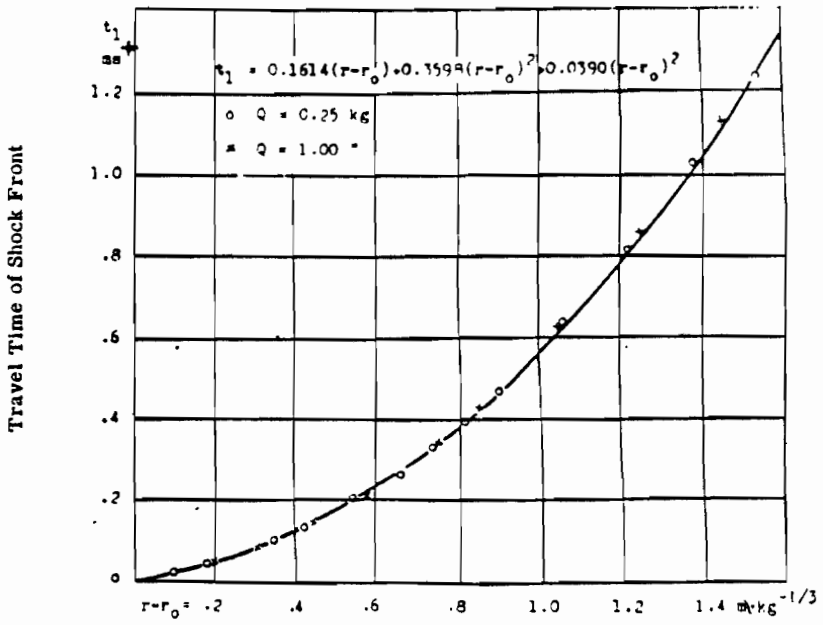

Travel Time of Shock Front

Distance from Charge Surface

Travel Times of the Shock Front from Different Explosives Compared to TNT at Various Distances from the Charge

FIG. 5

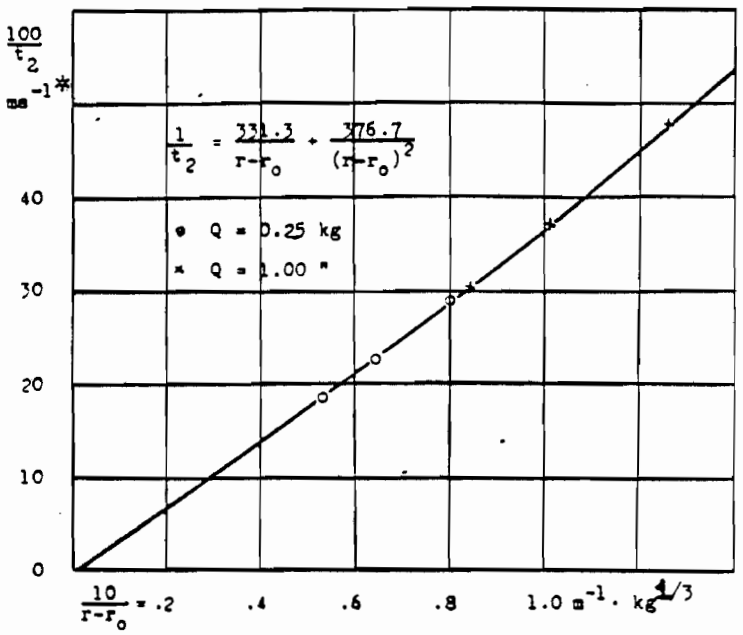

Reciprocal of Time at which Positive Phase Ends

Reciprocal of Distance from Charge Surface

Time at which Positive Phase Ends at Various Distances from Spherical TNT Charges.

+ [sic; ms · kg$^{-1/3}$]

* [sic; ms^{-1} · kg$^{1/3}$]

The derivatives $d\Delta/dr$ are determined by smoothing the measured values graphically.

Table IV presents the calculated values of travel times, velocities and wave-lengths for a spherical TNT charge at atmospheric pressure.

The measured travel times t_1 at various ambient densities of the air are evaluated according to Table III by comparison with the corresponding times for TNT calculated with the aid of the formulae mentioned before.

TABLE IV

CALCULATED TRAVEL TIMES, FRONT VELOCITIES, AND WAVE LENGTHS OF SPHERICAL TNT CHARGES AT ATMOSPHERIC PRESSURE

Values corrected to 1 kg charge weight, 0 deg C temperature, and 0 per cent humidity.

$r_o = 0.054$ m $kg^{-1/3}$.

$r - r_o$ m [1]	t_1 μs [2]	w_1 m·s^{-1}	$r - r_o$ m [1]	t_1 ms [3]	w_1 m·s^{-1}	t_2 ms [3]	l_+ ms [3]	l_+ m [4]
.00	0.0	6196	1.7	1.506	579.7			
.01	1.6	5931	1.8	1.682	558.0			
.02	3.4	5688	2.	2.052	523.6			
.03	5.2	5461	3.	4.186	425.7			
.04	7.0	5252	4.	6.80	388.0			
.05	9.0	5058	5.	9.25	371.3			
.06	11.0	4878	6.	11.95	362.1	15.22	3.27	1.08
.08	15.2	4551	8.	17.55	352.6	21.15	3.60	1.19
.10	19.7	4263	10.	23.27	347.8	27.10	3.85	1.27
.12	24.6	4009	12.	29.04	344.6	33.09	4.05	1.34
.16	35.2	3577	16.	40.68	341.3	45.09	4.41	1.46
.20	47.0	3226	20.	52.44	339.3	57.12	4.68	1.55
.24	60.0	2934	24.	64.25	338.0	69.16	4.91	1.63
.30	81.9	2579	30.	82.04	336.8	87.25	5.21	1.73
.40	124.7	2157	40.	111.82	335.5	117.40	5.58	1.85
.50	175.6	1817	50.	141.68	334.5	147.56	5.88	1.95
.60	234.7	1574	60.	171.59	334.0	177.73	6.14	2.03
.80	379.4	1232	80.	231.55	333.3	238.09	6.54	2.17
1.00	560.2	1002	100.	291.59	332.9	298.45	6.86	2.27
1.20	779.2	838	120.	351.70	332.6	358.81	7.11	2.36
1.60	1339.	620	160.	472.01	332.3	479.54	7.53	2.49
1.70	1506.	580	∞	∞	331.3	∞	∞	∞

1) [sic; m . $kg^{-1/3}$]
2) [sic; μs · $kg^{-1/3}$]
3) [sic; ms . $kg^{-1/3}$]
4) [sic; mm . $kg^{-1/3}$]

When $r - r_o \leq 1.70$, t_1 is calculated by the formula

$$t_1 = 0.1614\ (r - r_o) + 0.3598\ (r - r_o)^2 + 0.0390\ (r - r_o)^2.$$

(t_1 in milliseconds)

When $r - r_o \geq 1.70$, t_2 is computed by the formula

$$1/t_2 = 331.3/(r - r_o) + 376.7/(r - r_o)^2.$$

(t_2 in sec^{-1})

When $r - r_o \geq 12$, one has

$$w_1 = 331.3 + 160/r.$$

(w_1 in m sec^{-1})

The wave lengths are calculated by the approximate formula

$$l_+ = c_o t_+.$$

These dimensionless times are shown in Figure 6 as functions of $(r - r_o)$. For a given density ϱ_o the values apparently lie with sufficient accuracy on a straight line. Hence one may extrapolate with a satisfactory degree of precision to $(r - r_o) = 0$. Reciprocal values of the travel times for these values of ϱ_o give the ratio of the shock front velocity w_o at the density under consideration to the velocity at the normal density of 1.29 kg m^{-3} (see Figure 7).

It is apparent from Figure 8 [sic; Figure 7] that the relation between w_o and ϱ_o is practically linear and may be represented, if one chooses from Table IV the value $w_o = 6190$ m sec^{-1} for $\varrho_o = 1.29$, by the formula

$$w_o = 6190/(0.85 + 0.116\ \varrho_o).$$

(w_o in m sec^{-1})

for the range of ϱ_o from 1.29 to 5.1. The present experimental data are not yet sufficient to test whether the above formula holds also for the negative phase.

The travel times measured at atmospheric pressure for various explosives as given in Table III are also evaluated by direct comparison with TNT and plotted in Figure 8, which shows that the travel times and, therefore, also the shock front velocities of each explosive relative to TNT are not constant with respect to the distance $(r - r_o)$.

FIG. 6

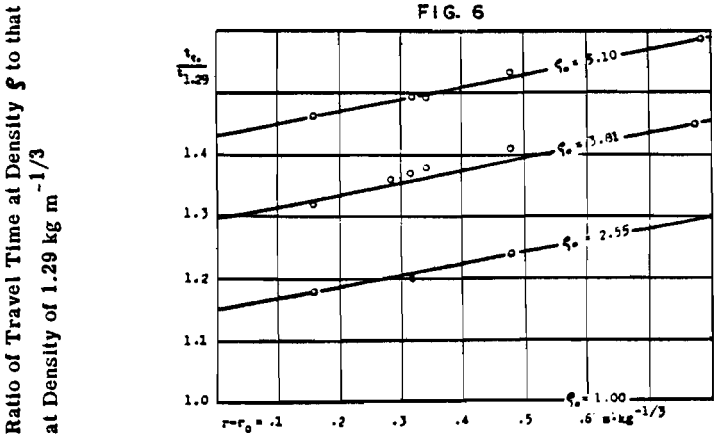

Distance from Charge Surface

Travel Time at Various Densities of the Surrounding Atmosphere at Various Distances from Spherical TNT Charges.

FIG. 7

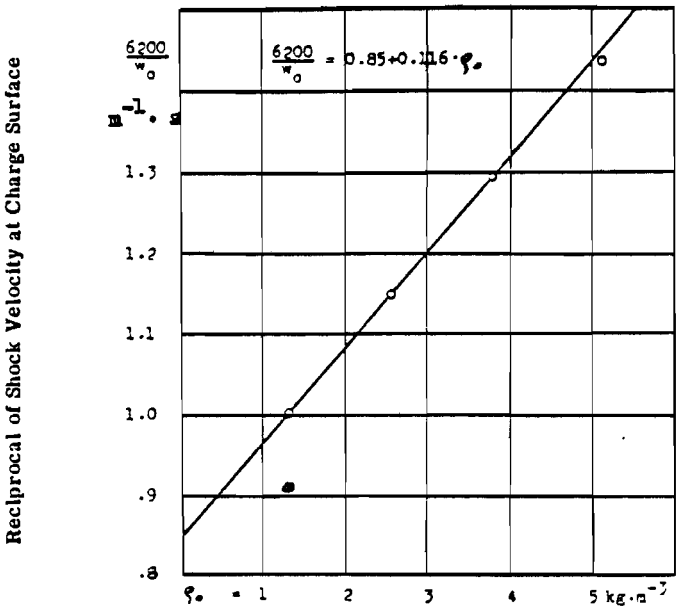

Density of Ambient Atmosphere

Front Velocity at the Surface of the Charge in Atmospheres of Various Densities.

FIG. 8

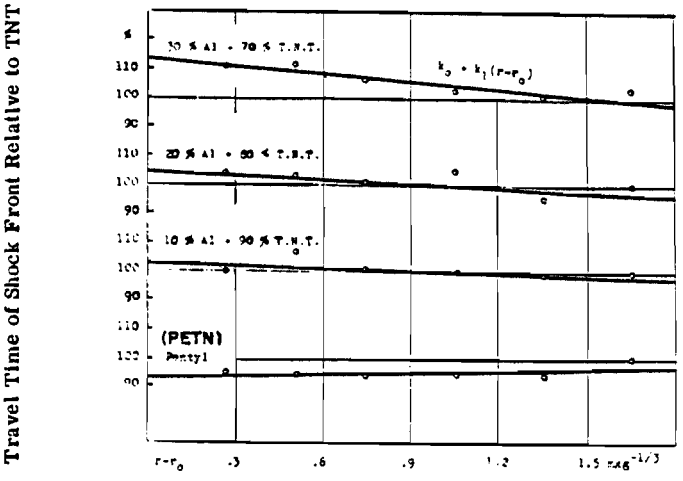

Distance from Charge Surface

Travel Time of the Shock Front at Various Distances from Spherical TNT Charges.

EXAMINATION OF RÜDENBERG'S AND SEDOV'S FORMULAE

According to Rüdenberg the shock front velocity w_o is calculated from the energy content E of the explosive charge, the specific density ϱ_o' of the distributed air, and the ambient density ϱ_o, by the formula

$$w_o = (E \varrho_o' / \varrho_o)^{1/2}.$$

Substituting values for TNT, this formula yields a value of w_o which is about one third of the measured value. For a given explosive ($E \varrho_o'$ constant) one should get

$$w_o \propto \varrho_o^{-1/2}.$$

The measured values for TNT do not obey this law at all. Neither does w_o change proportionally to $E^{1/2}$, according to experiments. Another method to approach this problem has been presented by the author elsewhere (Reference 8).

Rüdenberg gives for the relation between w_o and r

$$w_o = \left[a^2 (\chi + 1)/(\chi - 1) + (\chi - 1) \Sigma I/(8 \pi \varrho_o r^2) \right]^{1/2}.$$

Therefore, one should have for a given explosive and density

$$w_o^2 = a_1^2 + a_2/r^2$$

where a_1 and a_2 are constants. This means that w_o^2 should be a linear function of r^{-2}.

A graphical representation of these values according to Table IV does not verify this law.

Sedov gives (Reference 2) [Appendix A], using the same notation as above,

$$T_1 = (\varrho_o / E)^{1/2} \cdot R_5 \left[\text{sic; } (R^5 \varrho_o / E)^{1/2} \right].$$

Neither of the above dimensional formulae agrees with the measurements. This shows in addition that it is not possible to express T_1 as a product of unique functions, in the form $T_1 = f_1(\varrho_o) f_2(E) f_3(R)$, because for given values of ϱ_o and E, for example, the ratio of travel times for two different ambient densities, or for two different types of explosives, should be independent of r; i.e., each curve in both Figures 6 and 8 should be parallel to the $(r - r_o)$-axis, whereas actually they are not. Therefore, it is not possible to find a general distance law

$f_3(R)$ which is completely independent of the other parameters of explosion. This behaviour is explained by the fact that changes of the quantities describing the wave front are affected not only by the distance from the charge but also by the pressure distribution behind the front, as the author has shown elsewhere (Reference 9). This pressure distribution is not independent of the properties of the explosive material, and, therefore, each explosive substance must have its own characteristic pressure-distance law.

ACKNOWLEDGEMENT

All measuring equipment, with the exception of the spiral oscillograph and the tubes for the cathode-ray oscillograph, was designed and built by the Fysikaliska Forskingsavdelningen, AB Bofors. The measurements were made with great care by Engineer A. Häggkvist, who, furthermore, proposed and developed methods to provide the cathode-ray oscillograph with a PETN fuze and attended to the numerous important details.

SUMMARY

Travel times of shock waves emitted from bare spherical charges of high explosives have been measured. The experimental arrangements are described. Observed values may be reproduced with great precision by the formulae given in Figures 4 and 5.

The scaling laws have been verified over the whole range.

The relation between the front velocity and the ambient density of the surrounding atmosphere has been determined.

The front velocities of shocks from PETN and from different mixtures of TNT and Al have been determined (Figure 8).

The resulting data do not verify the theories of Rüdenberg and Sedov.

REFERENCES

1. Rüdenberg, R. — Über die Fortpflanzungsgeschwindigkeit und Impulsstärke von Verdichtungsstössen.

   Art. Monath., Vol. 113, 1918, pp. 237-265, and Vol. 114, 1919, pp. 285-316.

   [On the Velocity of Propagation and the Impulse of Shock Waves]

2. Sedov, L. I. — Le mouvement d'air en cas d'une forte explosion.

   C. R. Acad. Sci. URSS, Vol. 52, 1946, pp. 17-20.

   [The Motion of Air in a Strong Explosion]

3. Weibull, W. — Om den mekaniska verkan av brisanta sprängämnen vid detonation i luft och i vatten.

   Tidskr. Kustart., No. 2, 1944, pp. 3-35.

   [On the Mechanical Work of Explosives Detonated in Air and in Water]

4. Wolff, W. — Über die bei Explosionen in der Luft eingeleiteten Vorgänge.

   Ann. Phys. Chem., Vol. 69, 1899, p. 329.

   [On the Phenomena Induced by Explosions in Air]

5. v. Angerer, E., and Ladenburg, R. — Experimentelle Beiträge zur Ausbreitung des Schalles in der Freien Atmosphäre.

   Ann. Phys., Vol. 66, 1921, p. 293.

   [Experimental Contributions to the Propagation of Sound in Free Air]

6. Burlot, E. — Compte Rendu Sommaire des Expériences de La Courtine et des Essais qui les ont Précédées.

   Mém. Art. Franç., Vol. 4, 1925, pp. 479-523.

   [Summary Report on the Experiments at La Courtine and the Preceding Experiments at other Places]

7. Partlo, F. I., and Service, J. H. — Instantaneous speeds in air of explosion reports at short distances from the source.

   Physics, Vol. 6, 1925, pp. 1-5.

8. Weibull, W. Boundary Conditions at the Surface of Detonating High Explosives.

Ark. Mat. Astr. Fys., Vol. 34 B, No. 16, 1947.

9. Weibull, W. Ondes planes de pression à front discontinu.

VI^e Congr. Intern. Méc. Appl., Paris, 1946.

[Plane Shock Waves]

APPENDIX A

THE MOTION OF AIR IN A STRONG EXPLOSION

(Le movement d'air en cas d'une forte explosion)

by

L. I. Sedov

Comptes Rendus (Doklady) de L'Académie des Sciences de l'URSS
1946, Vol. 52, No. 1, pp.17-20

In my preceding communications (References A-1, A-2) I have shown certain new important families of solutions of non-linear equations in gas dynamics for plane, cylindrical and spherical waves. The gas motions corresponding to these solutions may have strong discontinuties which are propagated with variable velocity. The entropy, therefore, assumes different values for different gas particles.

It is of interest in the study of explosion phenomena to determine the law of variation of the shock wave velocity as a function of its position with respect to the place of explosion The shock wave velocity and the initial state of the gas determine the pressure jumps, the velocities and the densities of the gas particles; it is these magnitudes that should define the mechanical effect of the explosive action.

We shall now consider the problem of the propagation of an explosion wave under the following assumptions:

(1) In the spherical case one neglects the dimensions of the charge and we consider it as a point; the energy liberated by the explosion is regarded as finite.

(2) At the initial moment ($t = 0$) air is at rest. At the centre of explosion energy is released instantaneously and the air traversed by the shock front is disturbed.

(3) Atmospheric pressure is neglected relative to the shock front pressure.

The last assumption shows that the results of the solution do not depend on the initial pressure of the gas, but may depend on the initial density $\rho_0 \neq 0$ which characterizes the inertia of the gas particles.

The assumed ideal régime does not take into account factors which influence the phenomena taking place in the immediate vicinity of the charge (the finite dimension of the charge, the mass of the charge, etc.). At a large distance from the point of explosion the shock wave becomes a sound wave; in this process the atmospheric pressure is important and now the third assumption is inadmissible for the description of the phenomena at large distances from the charge.

The above assumptions may be considered reasonable where the shock is still strong but where the distance is large relative to the charge radius. Under such assumptions one may choose the following independent determinative dimensional parameters for the problem of adiabatic motion of an ideal gas:

the time t;

the coordinate r representing the distance from the point of explosion;

the atmospheric density ϱ_0,

a constant E, proportional to the energy liberated by the explosion.

One may modify the equation of motion and the equation of state of the gas to the system of independent quantities determining the dimension.

Now one may introduce different important physical constants the dimensions of which are expressible by the dimensions of E and of ϱ_0.

Having defined the system of characteristic parameters in this manner by means of dimension theory, it is simple to obtain the formulae which yield the laws of variation of the shock front velocity c and of the shock front distance r*.

In the spherical case one has

$$r^* = (E/\varrho_0)^{1/5}\, t^{2/5},\quad c = dr^*/dt = (2/5)(E/\varrho_0)^{1/2}\,(r^*)^{-3/2}; \tag{1}$$

similarly, in the cylindrical case

$$r^* = (E/\varrho_0)^{1/4}\, t^{1/2},\quad c = (1/2)(E/\varrho_0)^{1/2}\,(r^*)^{-1}; \tag{2}$$

and in the plane case

$$r^* = (E/\varrho_0)^{1/3}\, t^{2/3},\quad c = (2/3)(E/\varrho_0)^{1/2}\,(r^*)^{-1/2}. \tag{3}$$

It follows from the formulae (1), (2), and (3) that for differently shaped charges one obtains different laws of variation of the shock wave velocity with distance from the point of explosion.

At points behind the shock front we have

$$v = (r/t)\, V(\lambda),\quad \varrho = \varrho_0\, R(\lambda),\quad p = \varrho_0 (r/t)^2\, P(\lambda). \tag{4}$$

In the spherical case the abstract parameter λ is defined by the formula

$$\lambda = (E/\varrho_0)(t^2/r^5).$$

By (4) the problem of determining the motion of a gas may be reduced to one of ordinary differential equations. If the gas is ideal and the process adiabatic in the domain of continuous motion, the above equations become in the case of spherical symmetry (Reference A-2)

$$\frac{dz}{dV} = z\,\frac{\left[2(V-1)+3(\gamma-1)\right]\left(V-\frac{2}{5}\right)-(\gamma-1)V(V-1)\left(V-\frac{2}{5}\right)-\left[2(V-1)+\frac{6(\gamma-1)}{5\gamma}\right]z}{\left(V-\frac{2}{5}\right)\left[V(V-1)\left(V-\frac{2}{5}\right)+\left(\frac{6}{5\gamma}-3V\right)z\right]} \qquad (6)$$

$$\frac{d\ \ln\lambda^{1/5}}{d\ V} = \frac{\left(V-\frac{2}{5}\right)^2 - z}{V(V-1)\left(V-\frac{2}{5}\right)+\left(\frac{6}{5\gamma}-3V\right)z} \qquad (7)$$

$$\frac{d\ \ln\left(V-\frac{2}{5}\right)R}{d\ \ln\lambda^{1/5}} = \frac{3V}{V-\frac{2}{5}} \qquad (8)$$

where $z = \gamma P/R$ and $\gamma = c_p/c_v$, the ratio of the isobaric and isochoric heat capacities.

It may be shown that the system of equations (6), (7) and (8) possesses an integral

$$V^2\left(V-\frac{2}{5}\right)R + \frac{2}{\gamma-1}P\left(V-\frac{2}{5}\right) + 2PV = A\lambda \qquad (9)$$

where A is a certain constant.

To the state of imperturbed air corresponds a particular solution of the equations (6), (7) and (8) with $z = 0$; $V = 0$; $\rho = \rho_0$; $R = 1$ and λ arbitrary. Across the shock front the state changes abruptly and one has(Reference A-2)

$$\left.\begin{aligned} &V = 0.8/(\gamma+1);\ z = 0.32\,\gamma(\gamma-1)/(\gamma+1)^2 \\ &R = (\gamma+1)/(\gamma-1);\ \lambda = \text{const.} \end{aligned}\right\} \qquad (10)$$

The constant A vanishes for the state corresponding to the formulae (10). In this case the integral (9) leads to the following solution of equation (6)

$$z = \frac{(\gamma-1)(0.4-V)\,V^2}{2\left(V-\frac{2}{5}\gamma\right)}. \qquad (11)$$

To the centre of symmetry corresponds a particular solution of equation (6), namely

$V = 2/7$ and $z = \infty$.

Using (11), we may express λ and R in finite form as functions of V by starting from the equations (7) and (8). In this manner we obtain a simple and complete solution of the problem.

Figures A-1, A-2 and A-3 show the laws of variation of the velocity, the density and the pressure of air behind a shock wave ($\gamma = 1.4$); the constant E is related to E_1, the energy liberated by the explosion, by $E = 1.175\ E_1$.

At the centre of the explosion the velocity and the density are zero; the pressure approaches zero as the time increases. This shows that when a wave becomes weak an inverse motion of the gas toward the centre of the explosion must take place.

By means of the equations (6), (7) and (8) one may obtain the solution of (4) with several or even infinitely many shocks.

REFERENCES

(1) L. I. Sedov

On Unsteady Motions of a Compressible Fluid

C. R. Acad. Sci. URSS, Vol. 47, No. 2, 1945, pp. 91-93

(2) L. I. Sedov

Prikladnahya Matematika i Mekhanika, Vol. 9, No. 4, 1945.

FIG. A-1

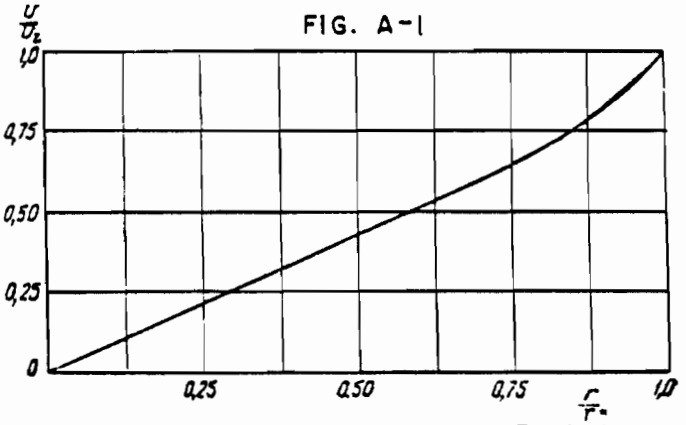

$\gamma = 1.4$: $E = 1.175\ E_1$; $v_2 = \frac{1}{3}\left(\frac{E}{\rho_0}\right)^{1/5} \frac{1}{t^{3/5}}$.

FIG. A-2

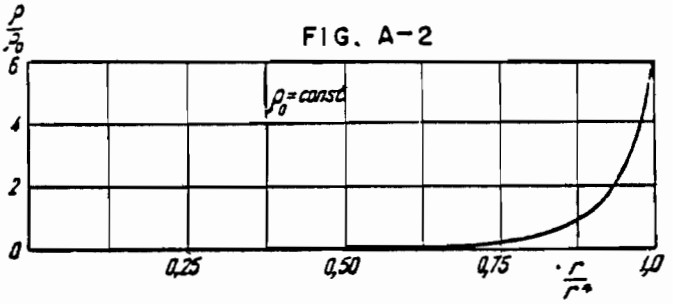

$r^* = \left(\frac{E}{\rho_0}\right)^{1/5} t^{2/5}$.

FIG. A-3

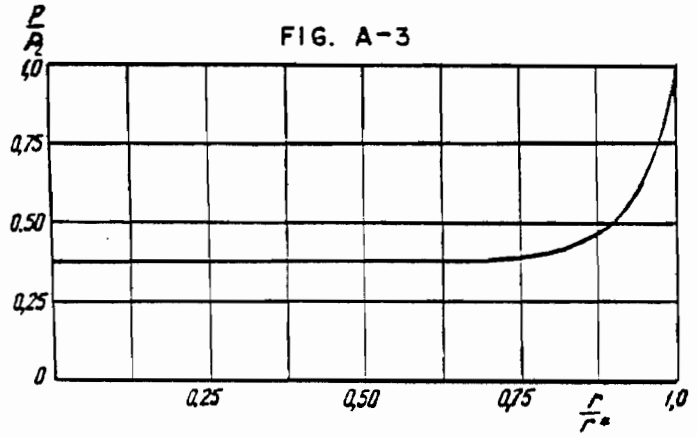

$p_2 = \frac{2}{15}\rho^{3/5} E^{2/5} \frac{1}{t^{1/5}}$.

APPENDIX B

COMPARISON WITH COMPILED DATA

Data on spherical Pentolite compiled at Aberdeen have been corrected from an assumed temperature of 20 deg C to 0 deg C and are plotted on Figure B as a smooth curve.

The corresponding part of Weibull's data on spherical TNT for Q = 0.25 kg as given in Table I is plotted on the same figure.

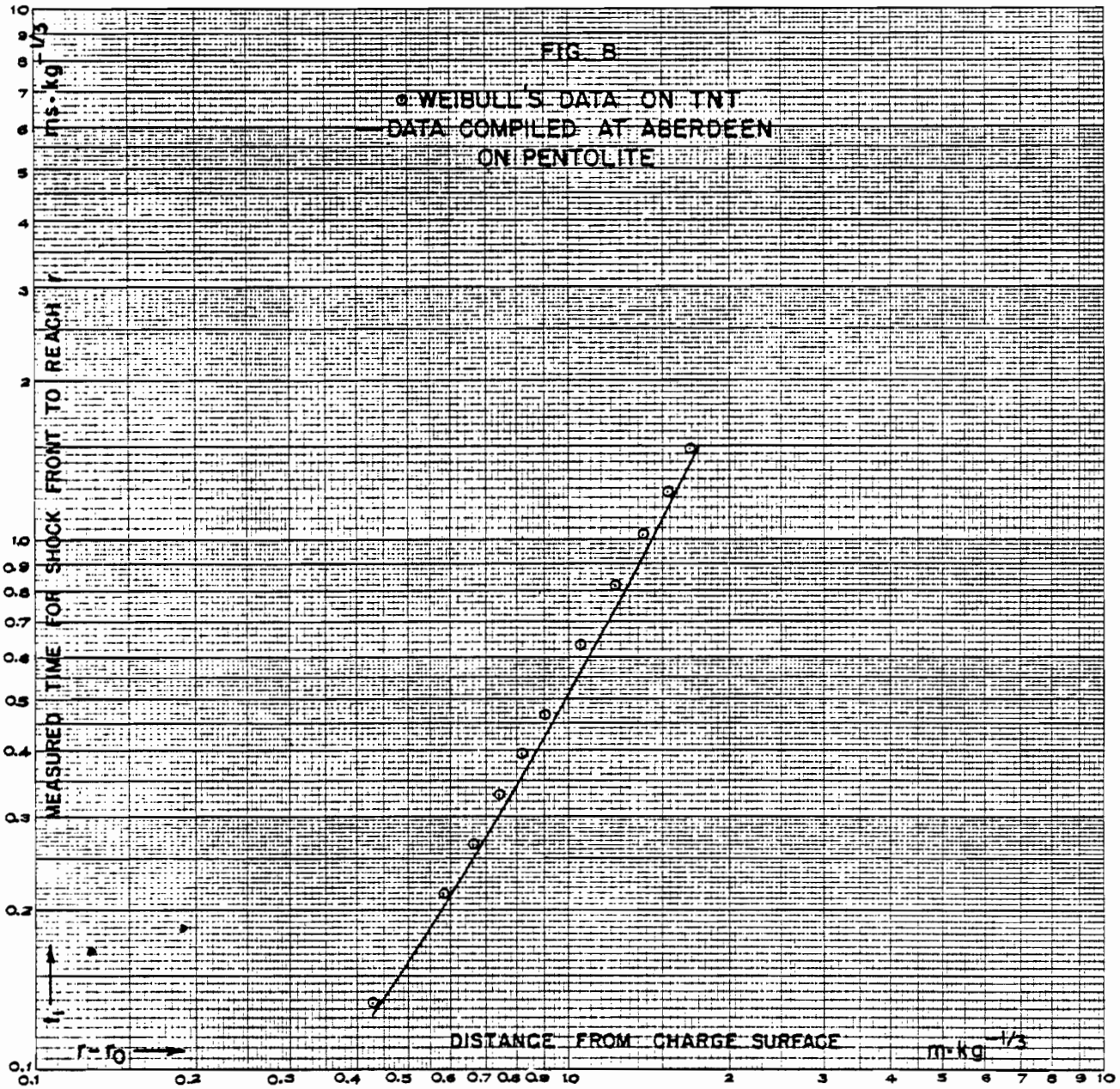

ARMY---OS---ABERDEEN PROVING GROUND, MD---139

DISTRIBUTION

No. of Copies	
4	Chief of Ordnance Washington 25, D. C. Attn: ORDTB-Bal Sec Mr. S. Feltman ORDTM Mr. H. S. Beckman Col. C. H. Roberts
6	British - 1 cpy of interest to ARE, Ft. Halstead Kent, England
1	Commanding Officer Naval Proving Ground Dahlgren, Virginia
1	Commander Naval Ordnance Laboratory White Oak Silver Spring 19, Maryland
1	Commanding Officer Naval Ordnance Test Station Inyokern, California P. O. China Lake, California Attn: Technical Library and Editorial Section
1	Bureau of Ordnance Navy Department Washington 25, D. C. Attn: Re3
1	Bureau of Aeronautics Navy Department Washington 25, D. C.
1	Commanding General Air Materiel Command Wright-Patterson Air Force Base Dayton, Ohio Attn: MCIDXD
1	Commanding Officer Naval Research Laboratory Anacostia Station Washington 20, D. C.

No. of Copies	
1	Dr. John von Neumann Professor of Mathematics The Institute for Advanced Study Princeton, New Jersey
1	Prof. G. B. Kistiakowsky Chemistry Department Harvard University Cambridge 38, Massachusetts
1	Dr. Bernard Lewis Chief, Explosives Branch U. S. Bureau of Mines Pittsburgh 13, Pennsylvania
1	Prof. Joseph E. Mayer Institute for Nuclear Studies University of Chicago Chicago 37, Illinois
1	Prof. Garrett Birkhoff Department of Mathematics Harvard University Cambridge, Massachusetts
1	Prof. Walker Bleakney Palmer Physical Laboratory Princeton University Princeton, New Jersey
1	Prof. Richard Courant Inst. for Mathematics and Mechanics New York University New York, New York
1	Prof. John C. Kirkwood Crellin Laboratory California Inst. of Tech. Pasadena 4, California
1	Prof. Walter S. Koski Department of Chemistry The Johns Hopkins University Baltimore, Maryland

No. of
Copies

1 Prof. R. Ladenburg
Palmer Physical Lab.
Princeton University
Princeton, New Jersey

1 Prof. Robert G. Sachs
Department of Physics
University of Wisconsin
Madison, Wisconsin

1 Dr. A. H. Taub
Department of Mathematics
University of Illinois
Urbana, Illinois

1 Chief of Engineers
Washington 25, D. C.

1 Major Bruce D. Jones
Protective Construction Br.
Office, Chief of Engineers
Washington, D. C.

1 Lt. Col. Max George
Armed Forces Special Weapons
Project
The Pentagon
Washington, D. C.

1 Dr. F. Reines
Los Alamos Scientific Lab.
Los Alamos, New Mexico

1 Dr. G. K. Hartman
Chief, Explosives Division
Naval Ordnance Laboratory
White Oak
Silver Spring, Maryland

1 Dr. E. F. Cox
Sandia Corporation
Albuquerque, New Mexico